Research Square

Preprints are preliminary reports that have not undergone peer review.
They should not be considered conclusive, used to inform clinical practice,
or referenced by the media as validated information.

Modelling and Optimization of TPH-Contaminated Soil Remediation Using Baobab Fruit Shell-Derived Biochar

Goziya William Dzarma

dzarmagoziya@yahoo.com

Chukwuemeka Odumegwu Ojukwu University (COOU)

Babayemi K. Akinpelu

Chukwuemeka Odumegwu Ojukwu University (COOU)

Umeuzuegbu C. Jonah

Chukwuemeka Odumegwu Ojukwu University (COOU)

Taitiya K. Yuguda

Admiralty University of Nigeria (ADUN)

Research Article

Keywords: Total petroleum hydrocarbon, remediation, sustainable, pyrolysis, optimization, modelling

Posted Date: November 26th, 2026

DOI: https://doi.org/10.21203/rs.3.rs-11498387/v1

License: This work is licensed under a Creative Commons Attribution 4.0 International License.
Read Full License

Additional Declarations: No competing interests reported.

Modelling and Optimization of TPH-Contaminated Soil Remediation Using Baobab Fruit Shell-Derived Biochar

Abstract

This research investigated the remediation of total petroleum hydrocarbon (TPH)-contaminated soil using biochar derived from baobab (*Adansonia digitata*) fruit shells. Key variables included remediation duration, biochar dosage, and initial pH levels. The biochar was produced via pyrolysis at 570 °C, exhibiting 69.30 wt% fixed carbon, 78.67 wt% elemental carbon, a specific surface area of 385.35 m^2/g, and a pore volume of 0.306 cm^3/g. Characterization methods, such as Fourier-transform infrared spectroscopy and scanning electron microscopy, revealed surface functional groups and porous structures conducive to enhancing TPH interactions. A response surface methodology (RSM) using a Box–Behnken design was utilized to optimize TPH removal, cation exchange capacity (CEC), and electrical conductivity (EC). The highest TPH elimination rate of 33.11% was observed after 12 days at a biochar dosage of 6 wt% and an initial pH of 7. CEC increased significantly from 18.04 to 66.75 cmol/kg, while EC escalated from 176 to 1353.45 µS/cm. The quadratic models showed excellent correlation with empirical data, boasting R^2 values of 0.9907, 0.9891, and 0.9901 for TPH elimination, CEC, and EC, respectively. Numeric optimization indicated an optimal remediation period of 20 days, a biochar application of 8.483 wt%, and a starting pH of 7.574, achieving projected results of 29.54% TPH elimination, 65.85 cmol/kg CEC, and 1353.45 µS/cm EC. The findings underscore the potential of baobab-derived biochar for remediating petroleum-contaminated soils while promoting the utilization of agricultural waste. It is recommended that further investigations into residual hydrocarbon toxicity be conducted prior to broader application.

Keyword: Total petroleum hydrocarbon, remediation, sustainable, pyrolysis, optimization, modelling

Goziya William Dzarma[1], Babayemi K. Akinpelu[1], Umeuzuegbu C. Jonah[1] and Taitiya K. Yuguda[2]

[1]Department of Chemical Engineering, Chukwuemeka Odumegwu Ojukwu University (COOU), Uli, Anambra State, Nigeria

[2]Department of Mechanical Engineering, Admiralty University of Nigeria (ADUN), Ibusa, Delta State, Nigeria.

Corresponding Author:
Goziya William Dzarma
dzarmagoziya@yahoo.com

Introduction

The soil embodies the Earth's vital epidermis, particularly as the uppermost stratum of the crust. The primary constituents comprise inorganic substances made up of diverse minerals and organic matter (OM), which encompasses a range of living microorganisms, in addition to air and water [1]. Recently, the escalating pollution of soils presents a considerable danger to the environment, agricultural yield, and human well-being [2]. Soil pollution due to total petroleum hydrocarbons (TPHs) is among the most prevalent forms of contamination globally, driven by the escalating demand for petroleum-derived energy and the massive extraction of petroleum products [3]. The European Environment Agency indicates that total petroleum hydrocarbons (TPHs) contamination accounts for over fifty percent of environmental liabilities, comprising mineral oils (23.8%), polycyclic aromatic hydrocarbons (10.9%), monoaromatic hydrocarbons (10.2%), halogenated hydrocarbons (8.3%), and heavy metals (35%) [4]. These contamination sources induce environmental imbalances, resulting in adverse economic and social consequences that diminish the value of the impacted regions. Conversely, the intrusion of contaminants into the soil allows them to access the aquifer utilized for public water supply, resulting in health issues [5], [6]. Consequently, the restoration of polluted soils is crucial for enhancing environmental quality and safeguarding human health.

As interest in soil remediation increases, various techniques have been suggested for locations contaminated with oil. Conventional, physical, and chemical soil remediation techniques are noted for their great efficacy in pollutant extraction and rapid decontamination duration. Nonetheless, physical and chemical techniques are costly, necessitate significant energy and labour expenditures, alter soil characteristics, and lead to secondary contamination. Biological cleaning procedures serve as an alternative to physical and chemical cleaning techniques [7]. Consequently, there is an immediate want for sustainable, economical, and scalable strategies to alleviate TPH contamination and safeguard agriculture and food security. Technologies centred on immobilization are unequivocally the foremost restorative strategy for soils tainted with TPH, and the application of carbon compounds, such as biochars (BC), is receiving heightened acknowledgement in this regard [2]. Biochar, a carbon-dense substance generated through the pyrolysis of organic biomass, has surfaced as a versatile instrument for sustainable environmental stewardship. Pyrolysis, a thermochemical procedure performed at temperatures ranging from 300 to 900°C in an oxygen-restricted environment, transforms agricultural byproducts, forestry debris, and various organic materials into a stable carbon form [8].

The ability of biochars to sustainably adapt into environmental management approaches has been attributed to a number of properties. Its porous composition, varied surface functional groups, and mineral constituents facilitate the adsorption of metals, organic pollutants, and nutrients, while simultaneously enhancing soil aeration, microbial activity, and water retention. Significantly, biochar functions as a durable carbon reservoir, in accordance with climate mitigation objectives [9], [10]. Moreover, due to its high organic

carbon concentration and resistance to biodegradation, biochar remains in the soil post-application, enhancing the organic matter content and thus improving the soil's physicochemical and biological characteristics [11]. The efficacy of biochar in many applications, including remediation, is contingent upon several aspects, such as the attributes of the biochar and the nature of the pollutants. The efficacy of the procedure is affected by various process variables including contact duration, pollutant concentration, pH levels, and biochar quantity. Therefore, there is a need to establish a robust relationship between the efficiency of biochar application and the influence of the controlling process parameters.

The conventional single-factor experimental approach analyses the influence of one variable on the response variable while maintaining other variables at a constant level. Despite its ease of use, this approach does not disclose the interactions between variables; also, as the number of variables increases, the quantity of tests grows exponentially, resulting in diminished optimization efficiency and the risk of missing the ideal process conditions [12]. Currently, statistical modelling and optimization methods have become effective instruments for modelling and improving intricate environmental processes, such as forecasting and augmenting biochar remediation efficacy. Response Surface Methodology (RSM) has been increasingly adopted for optimizing operational parameters in integrated systems, essential for comprehending the influence of process parameters in remediation [13]. RSM is a statistical and computational technique that employs factorial design to organize experiments, calibrate models, and ascertain optimal conditions for a desired result [14]. Present literary documents have reported the application of biochar from different biomasses in environmental remediation. However, there are no records of application of baobab fruit shell (BFS) derived biochar utilized in remediation of TPH polluted soil. In this regards, the current study seeks to model and optimize the TPH remediation efficiency and key soil parameters BFS derived biochar in the remediation of crude oil polluted soil.

Materials and Methods

Biochar production

The production of biochar was started by cleaning and preparing BFS, which was collected from the fruit processing site in Song Local, Adamawa State, Nigeria. The collected BFS sample was cleaned of fruit pulp strands, debris, and soil attachments and sun-dried for five (5) days. The dried biomass sample was milled to reduce the size to about 1-3 mm, after which it was weighed and oven-dried at the temperature of 80°C in order to determine moisture removed. The processed sample was packaged in an airtight container awaiting thermochemical conversion. 50 g of the processed BSF was carefully weighed and placed in a fixed-bed pyrolyzer. The setup was purged with nitrogen gas, circulated at 0.2 litres per minute, to ensure the process was carried out under inert conditions. The reactor was heated at a rate of 20°C/min, reaching a temperature of 570°C over a period of 2 hours. The reactor was allowed to cool completely, and the

resulting biochar was weighed and recorded. This process was carried out in triplicate, and the resultant yield of the pristine biochar was averaged.

$$yield\ of\ biochar = \frac{W_{BC}}{W_{BFS}} \times 100 - - - - - - - - - - - - - 1$$

Where W_{BC} represent the amount of biochar is produced and W_{BFS} is the amount of biomass feed into the reactor.

Biochar characterization

The produced biochar was characterized in order to establish a number of characteristic features. Proximate analysis was conducted, adopting standard procedures to determine the moisture content (ASTM D4442–07), ash content (ASTM D1102-84), volatile organic matter (ASTM D3175-11) and fixed carbon difference method, in accordance with conventional proximate analysis procedures. Using Elemental analyzer, elemental constituents nitrogen, hydrogen, and carbon were assessed in accordance with ASTM D5373-21 standards, while the sulphur content was measured utilizing ASTM D4239-11, and the oxygen concentration was derived by the difference method. Fourier Transform Infrared (FTIR) Spectroscopy to evaluate the chemical make up of the produced biochar. To determine the functional groups, 1g of the crystalline specimen was blended with potassium bromide (KBr, Merck for spectroscopy) and ground in an agate mortar until a fine, consistent powder was achieved. The uniform mixture was subsequently compressed to create translucent pellets appropriate for infrared transmission assessments. Spectral data were acquired via a PerkinElmer 3000 MX spectrometer across the spectrum of 4400–500 cm^{-1}. Each spectra was captured at a resolution of 4 cm^{-1}, use 32 scans per sample to guarantee consistency and reduce noise. A scanning electron microscope (SEM) (Jeol –JSM–7600F field) outfitted with energy-dispersive X-ray spectroscopy (EDS, 7021-H; HORIBA Co., Kyoto, Japan) was employed to examine the surface structure and elemental makeup of the collected biomass and biochar. The Brunauer–Emmett–Teller (BET) surface area assessments were conducted via N2 adsorption–desorption at 77 K utilizing a Micrometrics surface area analyzer (Model ASAP 2010, USA) to ascertain the surface area and pore size distribution of the adsorbent.

Soil sample collection and analysis

The crude oil contaminated soil was collected from a spill site in Ukwa East LGA of Abia State. Using soil auger, the collection was carried out at a depth of 15-30cm below the surface after clearing the collection site of surface debris. After collection at 5 different sites, the soil sample was combined for onward process at the laboratory, a process which involved removal of debris, air-drying for a five days and sieving to attain remove lumps. The processed soil sample was analyzed in order to determine a number of physicochemical properties. Standard procedures were employed to evaluate the physicochemical properties of the polluted soil, encompassing the determination of pH, moisture content (%), organic matter (%), organic carbon (%),CEC (cmol/kg), EC

(uS/cm), base saturation. Additionally, the TPH content of the polluted soil was obtained via extraction and the concentration determined gravimetrically using equation 2.

$$TPH\ \left(\frac{mg}{kg}\right) = \frac{W_e - W_f}{W_s} \times 10^6 \qquad 2$$

Where W_e is the weight of the extract and the flask before drying, W_f is the weight of the empty flask and W_s is the weight of the soil sample.

Soil remediation experiment

Experimental design

The soil remediation experiment was designed using Design Expert Version 13 (Stat Ease, Incorporated Minneapolis, MN, USA). Box–Behnken design (BBD) option of the response surface methodology (RSM) was adopted to establish the influence of three key process variables on the removal of TPH from the soil. The variables: time, biochar dosage, and initial pH were coded on three levels namely -1, 0, and +1. These designs are more economical than alternative 3k designs due to a reduced number of experimental trials. The equation for determining the quantity of experimental trials is N= 2k (k−1) + cp, where N denotes the number of trials, k signifies the number of factors, and cp indicates the count of replicates for the center points. All experimental data points constitute a hypersphere and maintain equal distance from the central point [15]. The design culminated in a total of 17 experimental trials conducted in a randomized manner to reduce systematic error [16]. The efficacy is quantified through the response (TPH removal efficiency, cation exchange capacity (CEC) and electrical conductivity (EC)) with the factor levels delineated by the design presented in Table 1.

Table 1: Range and level for process variables

Factor	Units	Factor Levels		
		-1	0	+1
Time	Days	4	12	20
Dosage of biochar	mg	0.2	0.6	1
Initial pH	-	3	7	11

Model development, statistical analysis and process optimization

The interaction between the process variables and their respective bearings on the response were modelled and statistically validated using analysis of variance (ANOVA) and relationship was fitted using a polynomial model presented in equation 3.

$$Y = \beta_o + \sum_{i=1}^{k} \beta_i X_i + \sum \sum_{i<j=3}^{k} \beta_{ij} X_i X_j + \sum_{i=j}^{k} \beta_i X_i^2 \qquad 3$$

Where Y is the response being studied, β_o and β_i are the regression model constants $X_i, X_j \; and \; X_i^2$ are the linear and polynomial coefficients of the process variables.

The optimization of the TPH removal efficiency, CEC, EC as well as the process variables was performed using the numerical desirability approach. The desirability function approach serves as an effective instrument for optimizing process factors. This method converts all acquired responses into a scale-invariant metric, spanning from 0 to 1, referred to as desirability. Values of 0 and 1 are assigned to represent the undesirability and optimality of responses generated by the process variables, respectively [17].

Remediation experiment procedure

In concordance with the design, 20g of the prepared soil specimen was meticulously measured and positioned in plastic containers (top diameter 15cm, bottom diameter 13cm, and height 6cm). Measure quantity of produced biochar was incorporated into each sampling container and properly blended to guarantee sufficient uniformity of the arrangement. Deionized water was incorporated into each setup and blended to achieve a moisture content of 50%. The initial pH of each setup was thereafter modified to correspond with the designed values utilizing HCl and NaOH solutions. The experimental arrangement was established in a ventilated area to closely resemble a natural environment. Following the designated timeframe, the individual setups were evaluated to ascertain the TPH, CEC and EC.

Results and discussion

Biochar characterization

Proximate and ultimate analyses

The findings of the proximate and ultimate analysis of the produced biochar is presented in Table 2. The low moisture content (1.72wt %) and volatile matter (10.83 wt %) observed in the produced biochar can be attributed to dehydration and devolatilization processes brought about by elevated temperature at which the thermochemical conversion is carried out. This result in the removal of moisture and the subsequent fragmentation of the volatile components into low-molecular-weight liquids and gases rather than biochar [18]. The fixed carbon content (69.30% wt%) and the amount of ash (18.13 wt%) present in the biochar is indicative of thermochemical transformation of the biomass resulting in gradual accumulation of inorganic components and organic matter combustion byproducts [19]. High levels of fixed carbon is attributable to decrease in volatile matter as a result of increasing temperature giving rise to more compact aromatic configurations and enhanced energy characteristics [20]. The elemental compositions, H/C and O/C ratios evaluated shows that the produced biochar is predominantly composed of elemental carbon (78.67%), reduced levels of oxygen (15.47% wt %) and hydrogen (2.60 wt %) respectively. Considering that the biomass is pyrolyzed at elevated temperature, such findings can be predominantly linked to dehydration, dehydrogenation, decarboxylation,

and dehydroxylation, this process entails the elimination of thermally unstable constituents from the biomass and the gradual condensation of aromatic carbon structures [21]. The O/C ratio of 0.15 falls short of the typical benchmark of 0.2 for very stable biochar, although the H/C ratio of 0.39 suggests a significantly carbonized composition. The comparatively low H/C and O/C atomic ratios of the biochar suggest a significant extent of carbonization throughout pyrolysis. The low value of H/C is due to ongoing dehydrogenation and the condensation of the carbon framework, while the diminished O/C ratio indicates the elimination of oxygenated groups by dehydration, decarboxylation, and decarbonylation processes. Reduced H/C and O/C ratios are typically linked to heightened aromaticity, hydrophobicity, carbon condensation, and enhanced resistance to chemical and microbial degradation [22].

Table 2: Proximate and ultimate analyses results

Proximate analysis	
Property	**(wt %)**
Moisture content	1.72
Volatile matter	10.83
Ash content	18.13
Fixed carbon	69.30
Ultimate analysis	
Element/Elemental ratio	**(wt %)**
Carbon (C)	78.67
Hydrogen (H)	2.60
Oxygen (O)	15.47
Nitrogen (N)	2.83
Sulphur (S)	0.35
H/C	0.39
O/C	0.15

Fourier transform infrared (FTIR) spectroscopy

The chemical composition of the generated biochar (BC) was analyzed using FTIR, and the resulting spectra are displayed in Figure 1. The FTIR spectra of the biochar generated at 570 °C displays multiple absorption characteristics throughout the analyzed wavenumber range, suggesting the existence of several surface functional groups and potential inorganic components. The extensive absorption area in the elevated wavenumber (3400–3500 cm^{-1}) spectrum could be linked to O–H stretching vibrations from hydroxyl groups and absorbed moisture, whereas the peak near 2924 cm^{-1} can signify remaining aliphatic C–H bonds [23]. The absorption band about 2368 cm^{-1} may be linked to ambient CO_2 interference and requires validation by background correction. The band at around 1629 cm^{-1} may be linked to aromatic C=C stretching or conjugated configurations, indicating the development of aromatic carbon regions during pyrolysis.

Absorption characteristics in the fingerprint region, especially near 1009, 915, and 753 cm^{-1}, could relate to C–O stretching and aromatic C–H deformation vibrations, albeit with potential overlapping influences [24]. The lower-wavenumber bands near 685, 546, and 468 cm^{-1} could signify vibrations associated with metal–oxygen and silicate from inorganic mineral components in the biochar.

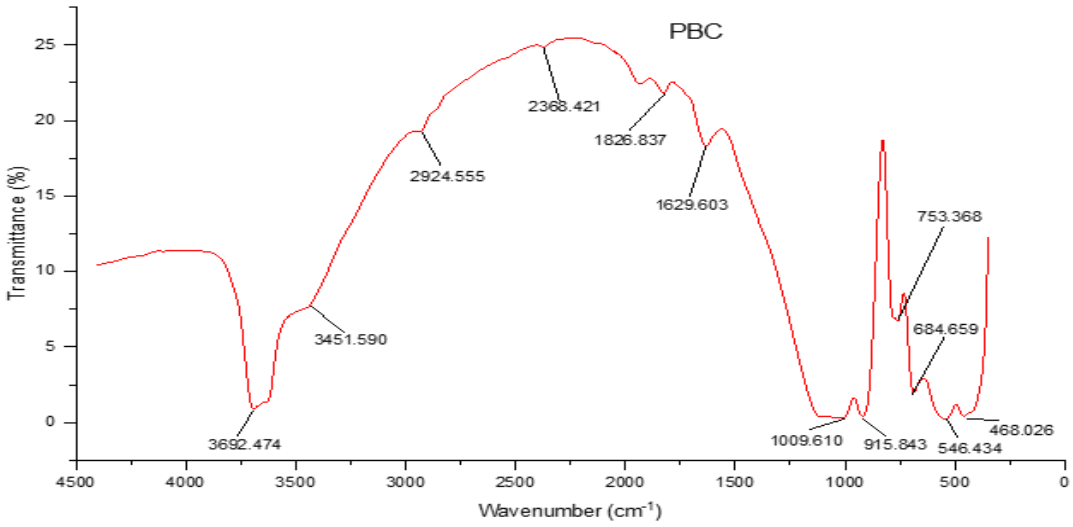

Figure 1: FTIR Spectrum of produced biochar

Scanning electron microscopy (SEM)

The SEM image of the produce biochar is presented in Figure 2. The SEM micrograph of BC displayed a diverse surface morphology marked by uneven carbonaceous formations, coarse surface characteristics, significant particle clustering, and discernible interparticle gaps. Significant pore voids arising from the heat decomposition of lignocellulose frameworks in the biomass during pyrolytic transformation, which resulted in the creation of porous cavities within the biochar. The heat breakdown of cellulose, hemicellulose, and lignin can modify the inherent structure of biomass, while the emission of volatile substances and the shrinkage of the solid framework may lead to the development of surface imperfections and cavities [25].

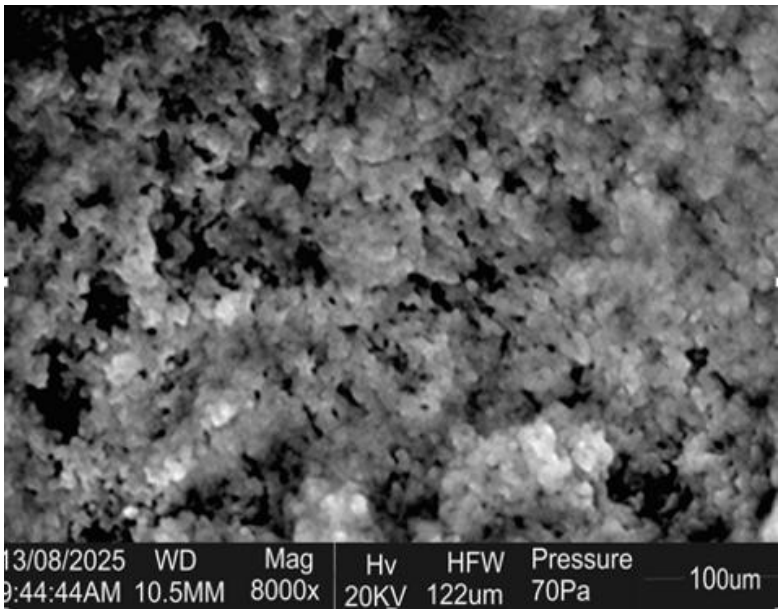

Figure 2: SEM Image of the produced biochar

BET analysis

The quantitative surface properties of the produced biochar, specific surface area (SSA), pore diameter (PD), and pore volume (PV) were evaluated using BET analysis. The results of the analysis are displayed in Table 3. The results indicate that the biochar generated at a high temperature (exceeding 500 ◦C) possesses a notable specific surface area of 385.35 m2/g. This discovery is due to the heightened temperature and prolonged duration, which augmented the probability of lignin decomposition, a principal element of the biomass utilized for biochar production [26]. Moreover, the generated biochar was found to exhibit a pore width of 2.07 nm, signifying a mesoporous configuration and an overall pore volume of 0.306 cm3/g. The availability of accessible active sites and the mesoporous characteristics of the biochar surface render it appropriate for the elimination of both organic and inorganic contaminants from the environment [27].

Table 3: Surface properties of produced biochar

Sample	SSA (m^2/g)	PD (nm)	PV (cm^3/g
BC	385.35	2.07	0.306

Soil sample analysis

The soil samples obtained for the investigation were meticulously processed and analyzed, with the findings presented in Table 4. The findings shows the soil is acidic, with a pH of 4.96 which can be attributed to the elevated level of TPH pollution recorded and the influence of petroleum hydrocarbons, potentially causing disruptions in gas exchange and the retention of carbon dioxide in the soil [28]. The organic carbon and organic matter contents of the TPH polluted soil were recorded as 14.60% and 25.17%

respectively, values that closely agree results reported by [29]. The moisture content in the soil sample was recorded to be 13.38%, which can be linked to the reduction in soil wettability brought about by presence of TPH in the soil [30]. The cation exchange capacity (CEC) of the soil sample was observed to be 18.04 cmol/kg, electrical conductivity (EC) was found to 176 uS/cm, exchangeable acidity (EA) was recorded as 8.45 cmol/kg and base saturation was observed to be 56.32 %.

Table 4: Physicochemical properties of TPH polluted soil

Property	**value**
pH	4.96
Organic carbon (%)	14.60
Organic matter (%)	25.17
Moisture content (%)	13.38
CEC (cmol/kg)	18.04
EC (uS/cm)	176
Exchangeable Acidity (cmol/kg)	8.45
Base Saturation	56.32
TPH (mg/kg)	98000

Soil Remediation

The soil remediation was carried out using the produced biochar in accordance with the designed BBD experimental approach and the findings of each experimental run is presented in Table 5.

Table 5: Summary of responses

Run	Factors			Responses		
	A:Time (Days)	B:Dosage (wt%)	C:pH	TPH Removal (%)	CEC (cmol/kg)	EC (µS/cm)
1	4	6	11	11.54	56.28	752.25
2	12	6	7	31.92	53.44	1158.35
3	4	2	7	17.73	39.73	519.17
4	20	6	11	24.77	58.16	1353.45
5	12	10	3	31.76	43.06	1106.03
6	20	10	7	28.14	66.75	1315.17
7	20	2	7	17.47	53.25	553.44
8	12	6	7	31.52	51.03	1193.17
9	12	6	7	31.85	50.24	1184.25
10	12	2	3	17.26	29.15	533.17
11	4	10	7	23.48	63.76	744.18
12	12	6	7	33.11	50.23	1134.35
13	12	6	7	31.27	51.89	1184.26
14	12	2	11	18.57	33.39	696.17

15	12	10	11	17.32	57.11	1227.13
16	4	6	3	28.28	43.71	722.98
17	20	6	3	24.13	49.87	855.83

The summary indicates that the minimum removal effectiveness of 11.54% occurred at a pH of 11, a biochar dosage of 6 wt%, and a duration of 4 days. The maximum reduction of TPH, at 33.11%, was seen after 12 days of remediation, utilizing an initial pH of 7 and a biochar dosage of 6 wt%. Adsorption of organic contaminants such as TPH is significantly influenced by the pH of the solution. At a neutral pH of 7, the surface charge of the biochar enhances physical adhesion and hydrophobic properties, ensuring the petroleum molecules remain securely attached to its porous structure. In contrast, a pH level of 11 that is strongly alkaline generates significant electrostatic repulsion forces and enhances the solubility or ionization of certain molecules, hence displacing hydrocarbons from the biochar pores and drastically reducing adsorption capacity [31]. The influence of the soil restoration process initiated by the incorporation of BC has been noted to enhance the CEC of the soil. The incorporation of biochar typically enhanced the cation exchange capacity (CEC) of the contaminated soil, with the most significant enhancement reaching 66.75 cmol/kg after 20 days, following the application of biochar at a concentration of 10wt% of the soil sample with an initial pH of 7.0. The obtained findings indicate a tendency to that observed in a study focused on improving the CEC of weathered soils via the incorporation of biochar by [32]. The electrical conductivity of the system exhibited a rising trend due to the incorporation of biochar together with the associated factors of time and initial pH. The maximum enhancement in the soil's electrical conductivity was noted at 1353.45 µS/cm with a biochar application of 6 wt%, an initial pH of 11, following a remediation duration of 20 days. Biochar frequently enhances electrical conductivity (EC) in soil due to its content of soluble mineral ash and exchangeable base cations, including Ca^{2+}, Mg^{2+}, K^{+}, and Na^{+}, which leach into the soil solution and elevate ionic conductivity [33].

Statistical modelling of remediation process

The experimental findings presented in Table 5 were modelled quadratically and validated statistically. The implication of each factor, independently and collectively on the responses based on ANOVA is presented in Tables 6, 7 and 8 respectively. Statistical significance of all model variables and responses were established on the confidence level of 95% level ($p < 0.05$).

Table 6: ANOVA Results for TPH removal efficiency

Source	Sum of Squares	df	Mean Square	F-value	p-value	
Model	754.30	9	83.81	82.64	< 0.0001	significant
A-Time	22.71	1	22.71	22.40	0.0021	
B-Dosage	110.04	1	110.04	108.50	< 0.0001	
C-pH	106.80	1	106.80	105.31	< 0.0001	
AB	6.05	1	6.05	5.97	0.0446	
AC	75.52	1	75.52	74.46	< 0.0001	
BC	62.02	1	62.02	61.15	0.0001	
A^2	90.58	1	90.58	89.32	< 0.0001	
B^2	131.61	1	131.61	129.77	< 0.0001	
C^2	110.19	1	110.19	108.66	< 0.0001	
Residual	7.10	7	1.01			
Lack of Fit	5.10	3	1.70	3.39	0.1343	not significant
Pure Error	2.00	4	0.5006			
Cor Total	761.40	16				
C.V. %	4.07					
Adequate Precision	25.9347					
R^2	0.9907					
Adjusted R^2	0.9787					
Predicted R^2	0.8888					

The ANOVA results presented the relationship between the model terms; time, biochar dosage, initial pH and the responses (TPH removal efficiency, CEC and EC) as a quadratic predictive equations. The model terms are represented as A, B and C in quadratic predictive models (Equations 4, 5, and 6). The contributory impact of the model terms, individually, combined and quadratically to the studied response are depicted by negative and positive signs showing decrease and increase in the respective responses examined.

$$TPH_{REff} = 31 + 1.69A + 3.71B - 3.65C + 1.23AB + 4.35AC - 3.94BC - 4.64A^2 - 5.59B^2 - 5.12C^2 \quad (4)$$

$$CEC = 51.37 + 3.07A + 9.39B + 4.89C - 2.63AB - 1.07AC + 2.45BC + 7.92A^2 - 3.41B^2 - 7.28C^2 \quad (5)$$

$$EC = 1170.88 + 167.41A + 261.32B + 101.37C + 134.18AB + 117.09AC - 10.47BC - 178.69A^2 - 209.19B^2 - 71.06C^2 \quad (6)$$

Table 7: ANOVA results for CEC

Source	Sum of Squares	df	Mean Square	F-value	p-value	
Model	1540.34	9	171.15	70.30	< 0.0001	significant
A-Time	75.34	1	75.34	30.95	0.0008	
B-Dosage	706.13	1	706.13	290.05	< 0.0001	
C-pH	191.59	1	191.59	78.70	< 0.0001	
AB	27.72	1	27.72	11.39	0.0118	
AC	4.58	1	4.58	1.88	0.2126	
BC	24.06	1	24.06	9.88	0.0163	
A^2	263.91	1	263.91	108.40	< 0.0001	
B^2	48.97	1	48.97	20.12	0.0028	
C^2	223.03	1	223.03	91.61	< 0.0001	
Residual	17.04	7	2.43			
Lack of Fit	9.79	3	3.26	1.80	0.2863	not significant
Pure Error	7.25	4	1.81			
Cor Total	1557.38	16				
C.V. %	3.12					
Adequate Precision	30.8035					
R^2	0.9891					
Adjusted R^2	0.9750					
Predicted R^2	0.8921					

From Tables 6-8, the F-values for TPH, CEC and EC were 82.64, 70.30 and 77.92, which shows that the model fit the experimental data adequately, implying that the predictors considerably account for variability in the responses recorded [17]. Additionally, for each of the developed predictive models, the lack of fit is not significant as indicated by p-value greater than 0.05. With these findings, there is sufficient proof indicating that the process variables significantly influence the various responses and that any residual variations in the obtained readings may be attributed to random error rather that model inadequacies. The developed predictive model was further evaluated for adequacy and accuracy using the coefficient of determination (R^2). From the analysis, the estimated R^2 of the models predicting TPH, CEC and EC were found to be 0.9907, 0.9891 and 0.9901, implying a very strong agreement between the experimental and the predicted values of the responses (Table 5). The adjusted R^2 (TPH = 0.9787, CEC = 0.9750 and EC = 0.9774) and the predicted R^2 (TPH = 0.888, CEC = 0.8921 and EC = 0.8667) respectively. These values close agree (as the variations between the two is less than 0.2), with adjusted R^2 compensating for inclusion of unwanted predictors and predicted R^2 depicting how well the model predict responses of new or unseen data [34]. This relationships are depicted graphically in Figure 3(a-c). The plots indicate a linear relationship between the actual

and the predicted data as the data points align along the diagonal, indicating the ability of the developed model to reproduce the experimental results adequately [35].

Table 8: ANOVA results for EC

Source	Sum of Squares	df	Mean Square	F-value	p-value	
Model	1.353E+06	9	1.503E+05	77.92	< 0.0001	significant
A-Time	2.242E+05	1	2.242E+05	116.25	< 0.0001	
B-Dosage	5.463E+05	1	5.463E+05	283.24	< 0.0001	
C-pH	82213.10	1	82213.10	42.63	0.0003	
AB	72017.09	1	72017.09	37.34	0.0005	
AC	54837.93	1	54837.93	28.43	0.0011	
BC	438.90	1	438.90	0.2276	0.6479	
A^2	1.344E+05	1	1.344E+05	69.71	< 0.0001	
B^2	1.843E+05	1	1.843E+05	95.53	< 0.0001	
C^2	21259.21	1	21259.21	11.02	0.0128	
Residual	13501.26	7	1928.75			
Lack of Fit	11155.20	3	3718.40	6.34	0.0532	not significant
Pure Error	2346.07	4	586.52			
Cor Total	1.366E+06	16				
C.V. %	4.60					
Adeq Precision	25.4568					
R^2	0.9901					
Adjusted R^2	0.9774					
Predicted R^2	0.8667					

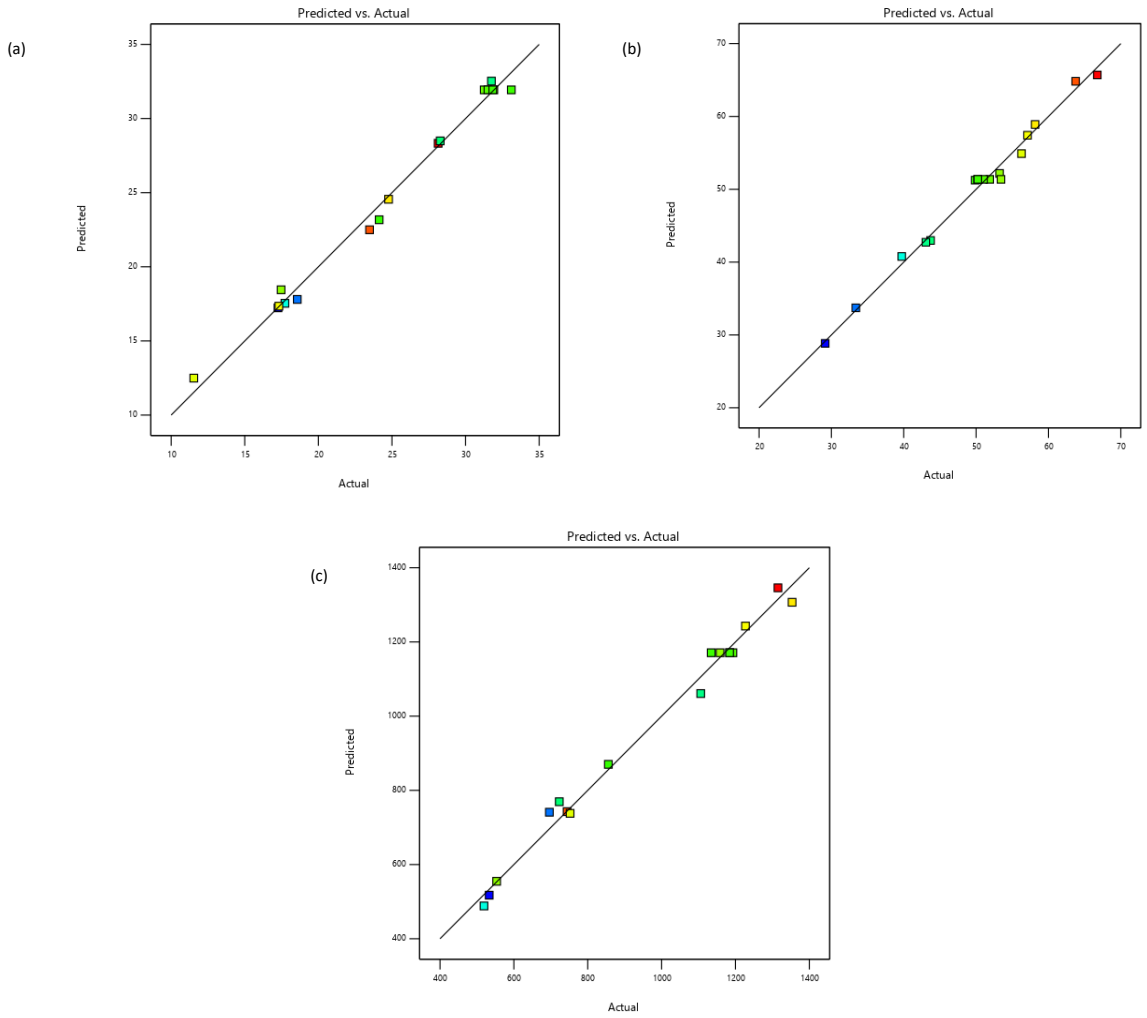

Figure 3(a-c): Plot of actual experimental and predicted data for (a) TPH (b) CEC and (c) EC

Interactive influence of process variables on the responses (TPH, CEC and EC)

TPH

The interaction between the process variables and the influence on the TPH remediation efficiency depicted in 3D plot is presented in Figure 4(a-c). From Figure 4a shows the interactive impact of time and biochar dosage on the response. Simultaneously increasing time and biochar shows that the efficiency of TPH removal increase up till an optimal level beyond which the effect becomes less significant. This is generally attributed to system saturation phenomena where the pore spaces are taken up, mass transfer limitations, or reduced incremental efficiency under elevated operational circumstances in environmental remediation systems [36]. As presented in Figure 4b, the 3D plot shows that increasing time and initial pH affect the TPH removal process, with a positive influence observed with respect time as compared to pH. However, a rise in the system's pH markedly diminished the TPH removal rate. This phenomenon can be ascribed to

modifications in the surface charge of the biochar, resulting in a variation in the adsorption rates of the intended pollutant [31]. The combined effect of biochar dosage and initial pH is presented in Figure 4c. The trend depicted in the plot indicate that increase both parameters simultaneously marginally increase the removal efficiency as shown by the contours.

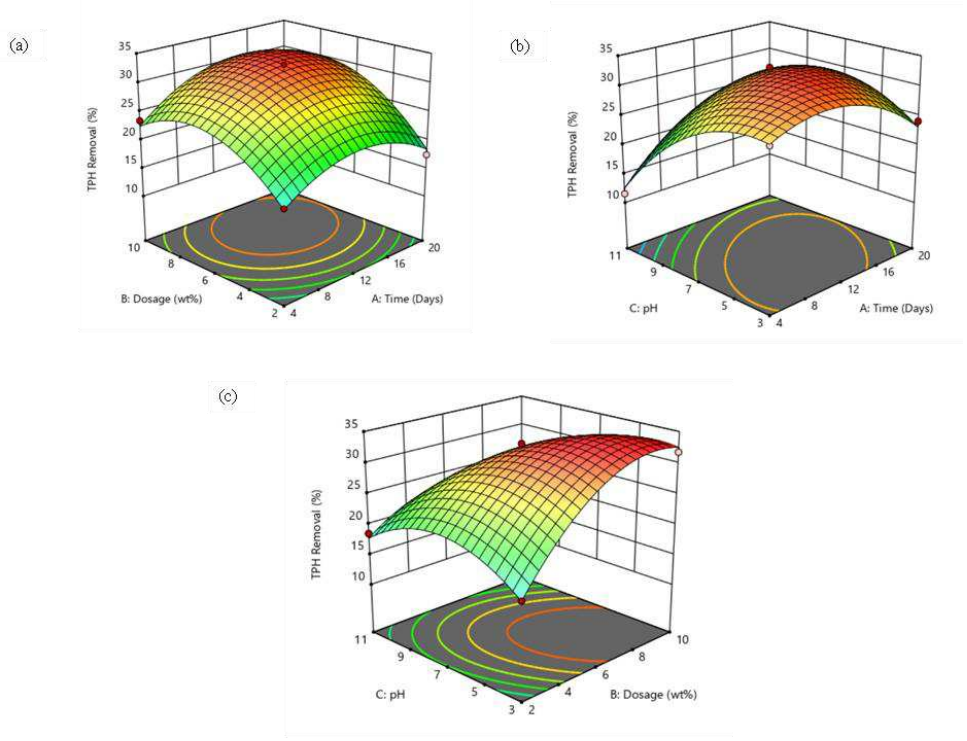

Figure 4(a-c): 3D Plot of process parameter interaction on TPH

CEC

The combined influence of the process variables on the CEC of the soil is presented in 3D plot in Figure 5(a-c). The interaction of time and biochar dosage as shown in Figure 5a present a trend of significant influence. The characteristics of the surface plot indicate that initial combinations of dosage and duration significantly impact the CEC, but further increases in either dosage or duration lead to a marked improvement in CEC. This interaction behaviour is probably due to the temporal physical and chemical maturation of the treatment media. At minimal dosages, the quantity of accessible active binding sites is intrinsically restricted, and brief durations fail to allow adequate time for the modification to interact with the matrix or form new functional groups. In contrast, with elevated dosages, the substantial quantity of the substance enables the system to surpass initial kinetic constraints. The extended timeframe probably aids in the gradual hydration, expansion, or chemical activation of the modification, revealing deeper interior surfaces and generating additional negatively charged functional groups (like carboxyl or hydroxyl groups) crucial for cation exchange [37], [38].

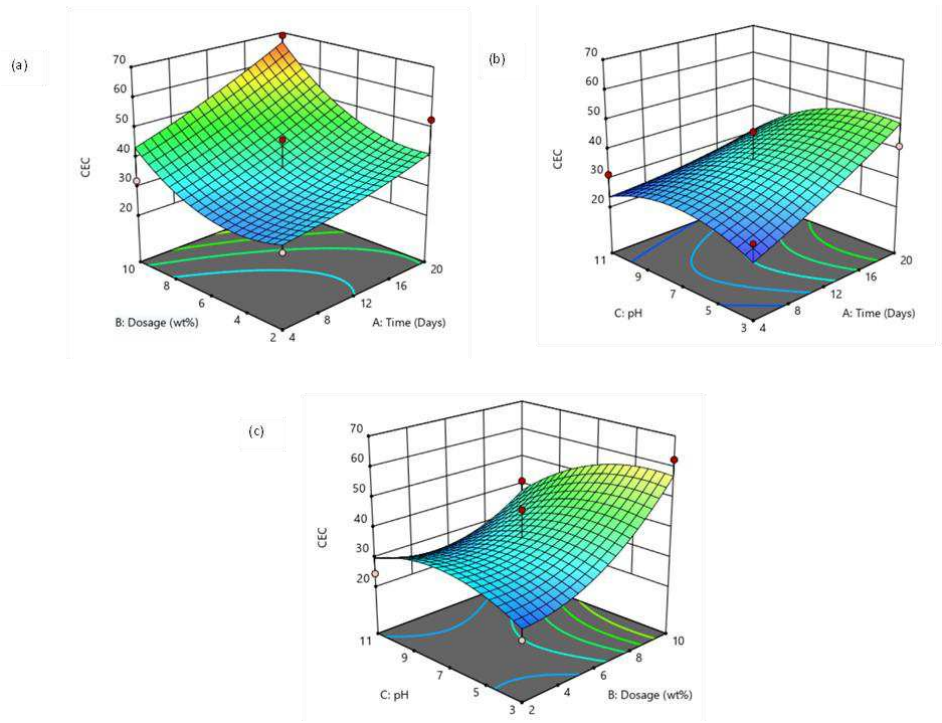

Figure 5(a-c): 3D plots of impact of process parameter interaction on soil CEC

The interaction between incubation time and initial pH on the CEC of the soil is present in Figure 5b. The shape of the plot indicate CEC typically rises with elevated pH and extended remediation duration, albeit the correlation is nonlinear. Within short treatment periods, CEC remains relatively low throughout the examined pH spectrum, but elevated CEC values are noted with increases in both pH and treatment duration. The response surface progressively ascends toward the area defined by elevated pH and extended treatment, suggesting that these circumstances enhance CEC. This conduct might be linked to pH-sensitive alterations in the surface charge and the accessibility of exchangeable sites in the biochar-soil system. Elevating pH can facilitate the deprotonation of oxygenated functional groups, thereby augmenting negatively charged sites that can hold and exchange cations. Extended treatment may facilitate increased interaction between biochar and the soil matrix, thereby augmenting the availability of exchange sites and improving cation retention [39]. The interactive influence of biochar dosage and pH on the response is presented in Figure 5c. The significant curvature of the response surface suggests a nonlinear association among pH, biochar dosage, and the cation exchange capacity (CEC) of the treated soil. CEC is considerably diminished in environments with lower pH and reduced biochar application, while increased values are noted in areas with higher pH and augmented biochar dose. This conduct can be ascribed to the synergistic impact of pH-sensitive surface charge and the role of biochar-derived exchange sites inside the soil matrix [40].

EC

The influence of process parameters in the experimentation of soil restoration was examined with respect to the soil EC and the trend is presented in 3D plots presented in Figure 6(a-c). The interaction of incubation time and biochar dosage as presented in Figure 6a shows that within the experimental range, EC increases with simultaneous increase in both parameters to an optimal point on the surface. The preliminary rise in electrical conductivity may be linked to the liberation of soluble and exchangeable ionic entities from the biochar into the soil solution. Biochar may encompass mineral ash and soluble salts that include ions like K^+, Ca^{2+}, Mg^{2+}, and several other inorganic entities, potentially elevating the concentration of charge-bearing ions in the soil solution and so improving EC. Augmenting the biochar dosage can thus incorporate a larger volume of these possibly soluble components. In a similar vein, extended contact duration may enhance the potential for the dissolution and mobilization of soluble mineral constituents from the biochar, facilitating their interaction with the soil solution and leading to elevated electrical conductivity [41].

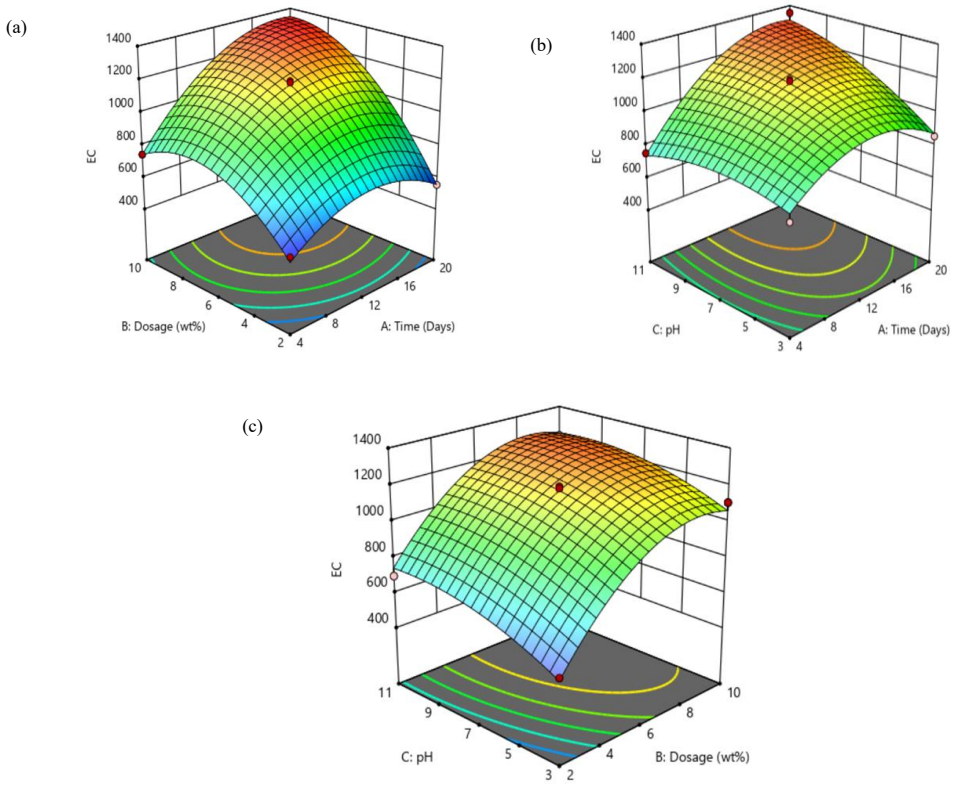

Figure 6(a-c): 3D plots of the interaction of process parameters and the influence on EC

The interaction between time and initial pH as presented in Figure 6b depict a similar trend indicating an synergistic interaction that influence the response to an optimal level before a decline is observed. This response is attributable to the same reason driving the response presented in Figure 5a. The interaction between initial pH of the system and

biochar dosage (Figure 6c) present a trend showing that more pronounced influence as a result of increasing dosage as compared to the initial pH of the system. This can be attributed to the fact that higher levels of biochar dosage can enhance soil pH by including alkaline mineral components, such as basic cations and carbonates, which aid in neutralizing soil acidity. Moreover, augmenting the biochar application rate could elevate electrical conductivity by liberating soluble mineral ions into the soil solution [42]. The interaction between biochar application rates and soil pH could so influence the variations in electrical conductivity.

Process optimization

The parametric factors examined in the remediation of TPH-contaminated soil were assessed to ascertain the highest achievable outcomes. To do this, the numerical optimization capabilities of Design Expert Version 13 (Stat Ease, Incorporated, and Minneapolis, MN, USA) were employed. The objective of the optimization was established to ascertain the values of the independent variables that concurrently maximize the responses. The importance of the process variables are weighted (lower and upper limits) as 1 and 3 respectively. The ideal process parameters for soil remediation were selected based on desirability values, employing the inherent desirability algorithm of the Design-Expert program. This approach facilitates the identification of ideal conditions for various factors concurrently by amalgamating separate desirability functions into a unified score. In practical application, the combined desirability value functions as a singular indicator that summarizes the system's performance across various objectives or responses [43].

The ramp results of the numerical optimization carried is presented in Figure 7. Based on the goal of the optimization, the maximized level of responses obtained shows that optimal parameters for optimal performance were determined to be a remediation duration of 20 days, a PBC dosage of 8.48336 wt%, and a pH of 7.5738. Under these circumstances, the highest TPH elimination rate achieved was 29.5353%, with CEC measured at 65.8527 cmol/kg and EC at 1353.45 µS/cm.

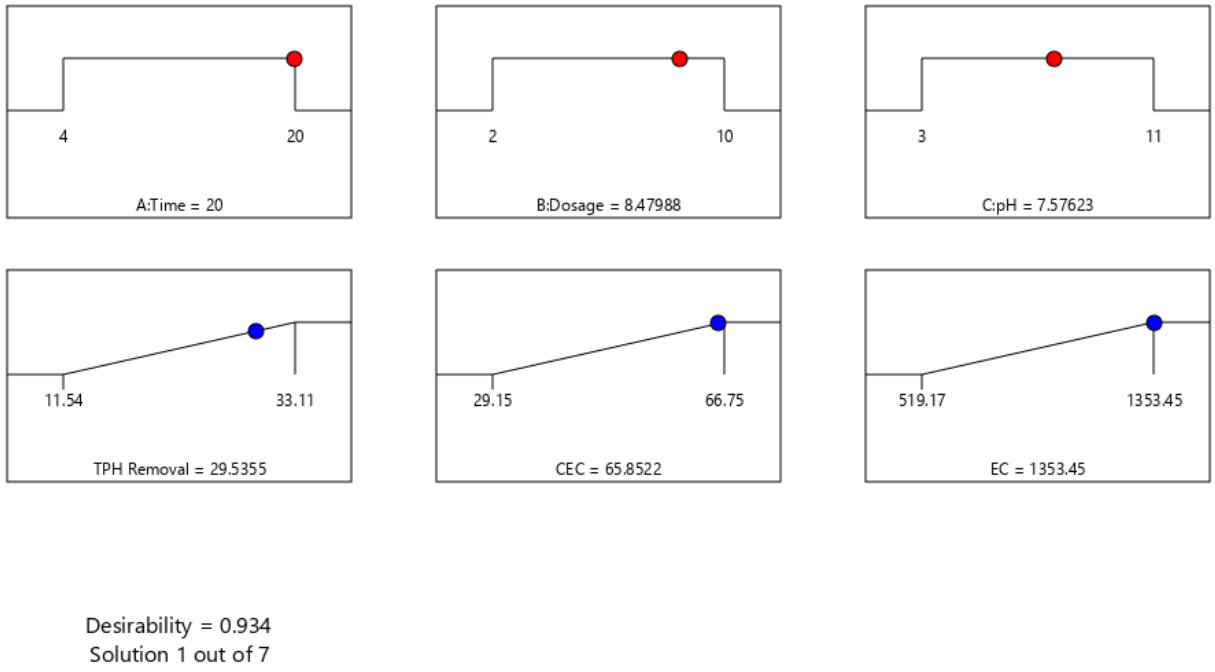

Figure 7: Numerical optimization result ramp

The desirability bar graph illustrating the process variables, the analyzed responses, and the aggregate for the optimal solution is displayed in Figure 8. The bar graph demonstrates that the independent variables analyzed in the study possess a desirability coefficient of 1, signifying that the chosen independent variables attained optimal overall performance in line with the optimization standards. Furthermore, the desirability of the solutions, both separately and together, approaches 1, signifying exceptional optimization efficacy [44].

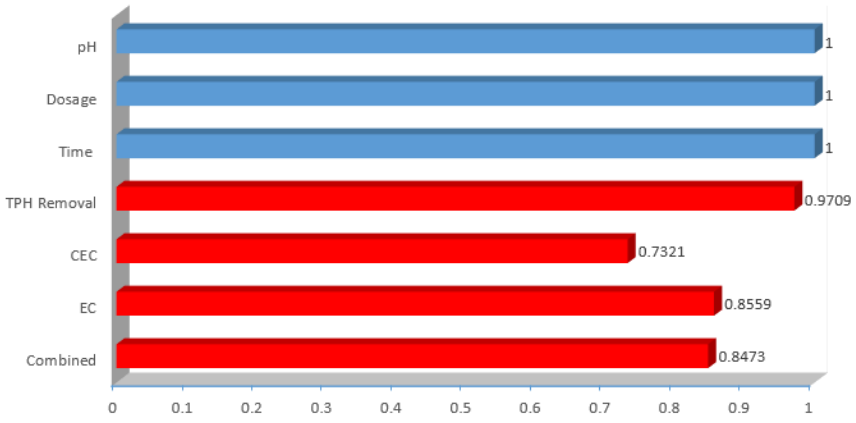

Figure 8: Desirability plot for the optimum parameters

Conclusion

The current study examined the efficacy of biochar sourced from baobab fruit shell (BFS) in the remediation of soil contaminated with total petroleum hydrocarbons (TPH), focusing on the effects of remediation duration, biochar application rate, and initial pH levels of the system. The remediation tests demonstrated that the removal of TPH was contingent upon the synergistic effects of the examined process parameters. The maximum experimentally recorded TPH elimination effectiveness was 33.11%, attained after 12 days with a starting pH of 7 and a biochar dosage of 6 wt%. The application of biochar also affected the physicochemical characteristics of the soil, enhancing the cation exchange capacity (CEC) from an initial measurement of 18.04 cmol/kg to a peak value of 66.75 cmol/kg. Electrical conductivity (EC) rose from 176 µS/cm to a peak of 1353.45 µS/cm, signifying the activation of soluble ionic components after the addition of biochar. Response surface methodology (RSM), utilizing a Box–Behnken design, effectively characterized the correlations between the process factors and the observed responses. The constructed models had elevated coefficients of determination (R^2) of 0.9907, 0.9891, and 0.9901 for TPH elimination, CEC, and EC, respectively, with no notable lack of fit. Numerical optimization determined that the ideal parameters for simultaneous response optimization are a remediation duration of 20 days, a biochar application rate of 8.48336 wt%, and an initial pH of 7.5738, resulting in projected values of 29.54% TPH elimination, 65.85 cmol/kg CEC, and 1353.45 µS/cm EC. In summary, biochar produced from baobab fruit shells presents a viable method for the valorization of agricultural waste and the remediation of petroleum-affected soils.

Funding Declaration: No funding was received during for this study

Ethics and Consent to Participate declarations: Not applicable

Data Availability Statement: The datasets generated during and/or analyzed during the current study are available from the corresponding author on reasonable request.

References

[1] T. Bousdra, S. G. Papadimou, and E. E. Golia, “The Use of biochar in the Remediation of Pb, Cd, and Cu-Contaminated Soils. The Impact of biochar Feedstock and Preparation Conditions on Its Remediation Capacity,” *Land*, vol. 12, no. 2, 2023, doi: 10.3390/land12020383.

[2] M. Raczkiewicz, D. Akachukwu, and P. Oleszczuk, “Sustainable soil remediation using nano-biochar for improved food safety and resource recovery,” *J. Hazard. Mater.*, vol. 494, no. March, p. 138537, 2025, doi: 10.1016/j.jhazmat.2025.138537.

[3] M. Rubežius, Ž. Kidikas, A. Kasiulienė, and V. Kemešytė, “Application of herbaceous plant mixtures for remediation of TPH-contaminated soil,” *Int. J. Phytoremediation*, vol. 27, no. 4, pp. 548–560, 2025, doi: 10.1080/15226514.2024.2427925.

[4] G. Caetano, R. D. M. Machado, M. Joana, N. Correia, I. M. Marrucho, and G. Caetano, “Remediation of soils contaminated with total petroleum hydrocarbons through soil washing with surfactant solutions soil washing with surfactant solutions,” vol. 3330, 2024, doi: 10.1080/09593330.2023.2198733.

[5] M. Chen, P. Xu, G. Zeng, C. Yang, D. Huang, and J. Zhang, “Bioremediation of soils contaminated with polycyclic aromatic hydrocarbons , petroleum , pesticides , chlorophenols and heavy metals by composting : Applications , microbes and future research needs,” *Biotechnol. Adv.*, vol. 33, no. 6, pp. 745–755, 2015, doi: 10.1016/j.biotechadv.2015.05.003.

[6] A. Karthick, B. Roy, and P. Chattopadhyay, “A review on the application of chemical surfactant and surfactant foam for remediation of petroleum oil contaminated soil,” *J. Environ. Manage.*, vol. 243, no. April, pp. 187–205, 2019, doi: 10.1016/j.jenvman.2019.04.092.

[7] U. Michael-igolima, S. J. Abbey, and A. O. Ifelebuegu, “A systematic review on the effectiveness of remediation methods for oil contaminated soils,” *Environ. Adv.*, vol. 9, no. November, p. 100319, 2022, doi: 10.1016/j.envadv.2022.100319.

[8] M. Ponraj, A. Murugan, and S. Alagendran, “The Role of Biochar in Soil Remediation and Carbon Sequestration,” vol. 12, no. 2, pp. 27–32, 2024.

[9] J. Dhiman, S. O. Prasher, E. Elsayed, R. M. Patel, C. Nzediegwu, and A. Mawof, “Environmental Technology & Innovation Heavy metal uptake by wastewater irrigated potato plants grown on contaminated soil treated with hydrogel based amendments,” *Environ. Technol. Innov.*, vol. 19, p. 100952, 2020, doi: 10.1016/j.eti.2020.100952.

[10] N. Uddin *et al.*, “Biochar – Hydrogel composites as multifunctional materials for environmental remediation and circular resource recovery,” *J. Hazard. Mater. Adv.*, vol. 22, no. March, 2026.

[11] Y. Dong, X. Guan, and H. Lin, “Biochar for simultaneous soil remediation and

carbon sequestration : application , mechanism , and development prospect – a comprehensive review," *Environ. Earth Sci.*, vol. 85, no. 98, 2026.

[12] C. Liu *et al.*, "Response Surface Methodology for Biochar Performance Optimization : A Comprehensive Bibliometric Review," pp. 1–33, 2026.

[13] D. Hogan and N. Uzor, "Modelling and Optimizing the Effect of pH on Remediation of Crude Oil Polluted Soil with Biochar Blend : RSM Approach," vol. v, no. 3, pp. 56–73, 2023, doi: 10.9734/AIR/2023/v24i3942.

[14] H. Chen and C. Chen, "A Study of the Response Surface Methodology Model with Regression Analysis in Three Fields of Engineering," pp. 1–32, 2025.

[15] G. W. Dzarma, B. K. Akinpelu, and U. C. Jonah, "South African Journal of Chemical Engineering Parametric modelling and optimization of biochar production from baobab fruit shell using response surface methodology," vol. 57, no. December 2025, 2026.

[16] A. S. Yusuff, N. B. Ishola, A. O. Gbadamosi, and E. I. Epelle, "Modeling and Optimization of Hexavalent Chromium Adsorption by Activated Eucalyptus Biochar Using Response Surface Methodology and Adaptive Neuro-Fuzzy Inference System," 2023.

[17] O. Adeyi *et al.*, "Sequential optimization of drying and extraction processes for enhanced antioxidant recovery from Parquetina nigrescens leaves: Assessing drying parameters and extraction model reliability," *Can. J. Chem. Eng.*, vol. 1, no. February, pp. 1–21, 2025, doi: 10.1002/cjce.25773.

[18] A. Tomczyk, S. Zofia, and B. Patrycja, "Biochar physicochemical properties : pyrolysis temperature and feedstock kind effects," *Rev. Environ. Sci. Bio/Technology*, vol. 19, no. 1, pp. 191–215, 2020, doi: 10.1007/s11157-020-09523-3.

[19] M. K. Rafiq, R. T. Bachmann, M. T. Rafiq, Z. Shang, S. Joseph, and R. Long, "Influence of Pyrolysis Temperature on Physico-Chemical Properties of Corn Stover (Zea mays L .) Biochar and Feasibility for Carbon Capture and Energy Balance," pp. 1–17, 2016, doi: 10.1371/journal.pone.0156894.

[20] A. D. S. Borges, M. Cardoso, and M. Oliveira, "Thermochemical evaluation of biochars properties from Portuguese agro-forestry residues for solid fuel applications," pp. 1–14, 2026.

[21] M. Bivareh, N. Mahmoudi, H. Younesi, and O. Safari, "Effects of feedstock and pyrolysis temperature on carbon stabilization and mineral functionality of biochars," *Sci. Rep.*, 2026.

[22] J. A. Ippolito, L. Cui, C. Kammann, N. Wrage, and M. Jose, "Feedstock choice , pyrolysis temperature and type influence biochar characteristics : a comprehensive meta - data analysis review," *Biochar*, vol. 2, no. 4, pp. 421–438, 2020, doi: 10.1007/s42773-020-00067-x.

[23] A. M. Atoshi, G. Boro, M. Jimwan, and F. S. Comfort, “Thermal, Structural and Flammability Characteristics of Polypropylene Composites Reinforced with Untreated Canarium schweinfurthii Nut-Shell Particles,” *Kwaghe Int. J. Sci. Technol.*, vol. 3, no. 3, pp. 487–505, 2026.

[24] J. Kujawska, W. Cel, and B. Charmas, “Effect of Pyrolysis Temperature on Chemical Structure and Thermal Stability of Digestate-Based Biochar,” pp. 1–20, 2026.

[25] P. R. Yaashikaa, P. S. Kumar, S. Varjani, and A. Saravanan, “A critical review on the biochar production techniques , characterization , stability and applications for circular bioeconomy,” *Biotechnol. Reports*, vol. 28, p. e00570, 2020, doi: 10.1016/j.btre.2020.e00570.

[26] E. B. Dayoub, Z. Tóth, G. Soós, and A. Anda, “Chemical and Physical Properties of Selected Biochar Types and a Few Application Methods in Agriculture,” *Agron. Rev.*, vol. 14, no. 24500, 2024.

[27] D. S. Thakur and S. N. Chadar, “Synthesis and Characterization of Coconut Shell-Based Nanobiochar Produced by Controlled Pyrolysis for Dye Adsorption from Wastewater,” *Res. Dev. Mater. Sci.*, vol. 22, no. 2, 2025, doi: 10.31031/RDMS.2025.22.001034.

[28] M. Cheraghi, S. Soheil, L. Bahareh, M. Hajar, M. H. Parvizi, and 1, “Biochemical and Physical Characterization of Petroleum Hydrocarbon Contaminated Soils in Tehran,” vol. 5, pp. 199–208, 2015.

[29] U. P. Ojukwu and A. N. Eboatu, “Assessment of Physicochemical Parameters of Soils Contaminated with Petroleum from Eleme Port Harcourt , Nigeria,” *Int. J. Eng. Res. Sci.*, vol. 8, no. 11, pp. 7–11, 2022.

[30] T. Saikia, J. Bora, and C. Gogoi, “Impact of Crude Oil Contamination on Soil Physicochemical Properties around the Sildubi Oil Spill , Borhola , Assam,” vol. 35, no. 22, pp. 241–253, 2023, doi: 10.9734/IJPSS/2023/v35i224130.

[31] C. Ji, H. Yin, M. Zhou, and Z. Sun, “Adsorption of total petroleum hydrocarbon in groundwater by KOH-activated biochar loaded double surfactant-modi fi ed nZVI,” *Front. Mater.*, vol. 10, no. September, pp. 1–15, 2023, doi: 10.3389/fmats.2023.1234981.

[32] R. R. Domingues *et al.*, “Enhancing Cation Exchange Capacity of Weathered Soils Using Biochar : Feedstock , Pyrolysis Conditions and Addition Rate,” *MDPI Agron.*, vol. 10, no. 824, pp. 1–17, 2020.

[33] S. Thallapally, S. Chepyala, J. Bathula, S. Mudalkar, and S. Eetela, “biochar on the physicochemical and fertility properties of industrial acidic soil,” 2026.

[34] D. Chicco, M. J. Warrens, and G. Jurman, “The coef fi cient of determination R-squared is more informative than SMAPE , MAE , MAPE , MSE and RMSE in regression analysis evaluation,” pp. 1–24, 2021, doi: 10.7717/peerj-cs.623.

[35] K. O. Jimoh *et al.*, “Concrete water cement ratio prediction system using random

forest regression," *Discov. Concr. Cem.*, 2025, doi: 10.1007/s44416-025-00005-9.

[36] C. Djelloul, A. Hasseine, and O. Hamdaoui, "Adsorption of cationic dye from aqueous solution by milk thistle seeds : isotherm , kinetic and thermodynamic studies," vol. 78, pp. 313–320, 2017, doi: 10.5004/dwt.2017.20920.

[37] A. I. Osman, E. M. Abd, E. Monaem, A. M. Elgarahy, and C. O. Aniagor, *Methods to prepare biosorbents and magnetic sorbents for water treatment : a review*, vol. 21, no. 4. Springer International Publishing, 2023. doi: 10.1007/s10311-023-01603-4.

[38] V. Tsolis, "Biochar as Soil Amendment : The Effect of Biochar on Soil Properties Using VIS-NIR Diffuse Reflectance Spectroscopy ," 2023.

[39] J. N. Nkoh *et al.*, "A Critical-Systematic Review of the Interactions of Biochar with Soils and the Observable Outcomes," 2021.

[40] L. Du *et al.*, "Evolution of Biochar Structure and Its Impact on Volatile Adsorption and Reforming during," pp. 1–21, 2025.

[41] X. Teng *et al.*, "Effects of biochar on soil properties as well as available and TCLP- extractable Cu contents : a global meta-analysis," *Sci. Rep.*, vol. 15, no. 32853, pp. 1–12, 2025.

[42] V. Y. Adam and E. Erhus, "COMMUNITY MEDICINE AND One-year prevalence of domestic violence against women during the COVID-19 pandemic in an urban community in Southern Nigeria," *J. Community Med. Prim. Heal. Care.*, vol. 34, no. 1, pp. 117–130, 2022.

[43] V. Marinkovi, "Some Applications of a Novel Desirability Function in Simultaneous Optimization of Multiple Responses," *FME Trans.*, vol. 49, pp. 534–548, 2021, doi: 10.5937/fme2103534M.

[44] A. Y. Şeflek, N. Orhan, and M. Özkan, "The impact of tractor drawbar height on performance and optimization using response surface methodology," pp. 1–14, 2025.